PHOTOELECTRONICS

UDC 621. PACS: 85, 85.60.–q
EDN: GETOGH

Uncooled photosensor array 640×512 with an extended sensitivity range of 0.4–2.0 μm based on colloidal quantum dots PbS CQDs with an electron-blocking *p*-NiO$_x$ layer

© V. P. Ponomarenko[1,2], V. S. Popov[1,2,*], M. A. Pankov[1], K. A. Khamidullin[1], A. D. Deomidov[1], A. A. Fedorov[1], G. Yu. Deev[1], D. E. Dragunov[1], O. V. Epifanov[1], P. I. Zaripov[1], P. S. Lazarev[1], E. V. Mirofyanchenko[1], D. V. Ilyinov[1], V. A. Petrushina[1], I. D. Burlakov[1], A. V. Polessky[1], V. V. Startsev[1], S. B. Brichkin[2,3], M. G. Spirin[2,3], S. A. Tovstun[2,3], M. V. Gapanovich[2,3], V. Yu. Gak[2,3], A. V. Gadomskaya[2,3], D. N. Pevtsov[2], A. V. Katsaba[2], A. S. Kirichenko[2], D. V. Dyomkin[2], V. A. Ivanova[2], V. V. Ivanov[2], V. F. Razumov[2,3]

[1] RD&P Center ORION, JSC, Moscow, 111538 Russia
[*] E-mail: popov.vs@mipt.ru
[2] Moscow Institute of Physics and Technology (National Research University), Moscow Region, Dolgoprudny, 141701 Russia
[3] Federal Research Center for Problems of Chemical Physics and Medicinal Chemistry of the Russian Academy of Sciences Moscow Region, Chernogolovka, 142432 Russia

Received 03.03.2025; revised 25.03.2025; accepted 07.04.2025
Scientific specialty code: 1.3.11

Night vision devices with an extended sensitivity range of 0.4 μm to 2.0 μm are essential for scientific, civil and special-purpose applications. The architecture and basic specifications of the array photosensor of the 640×512 format (15 μm pitch) with the extended sensitivity range (0.4-2.0 μm) developed on the basis of PbS CQP colloidal quantum dots are described. The major part of the photocurrent is generated in CQD layer n-PbS-TBAI. The layer has been made by substituting the initial ligand (oleic acid) with iodine during treatment of the CQD layer with tetra-n-butylammonium iodide (TBAI). The electron-blocking layer (hole transport layer) has been created on the basis of p-NiO$_x$. The hole-blocking layer (electron transport layer) has been created on the basis of n-ZnO.

Keywords: colloidal quantum dot (CQD); ligand; transport layer; photosensor.

DOI: 10.51368/1996-0948-2025-2-12-20

1. Introduction

The recent period has been marked by the rapid growth in the research aimed at creating array photosensors (FPA) using materials and structures of limited dimensions [1–3]. A new trend in the field of photosensors can be clearly seen in the last two decades. This trend is associated with the use of so-called quasi-zero-dimensional colloidal quantum dots (CQDs), the spectral properties of which are determined by the average size of semiconductor nanoparticles that vary within the range of 2–10 nm. The development of this direction led to the creation in 2020 of the first serial-producted matrices and cameras that are based on CQDs and operate in the spectral range from 0.4 to 2.1 μm [3].

The use of colloidal quantum dots allows to significantly simplify the technology, relieve the limitations imposed on the pitch of photosensitive elements [4] and significantly decrease the FPA cost [5].

The technology of manufacturing array photosensors using CQDs, which was named the monolithic-hybrid technology [4, 6], is based on application of liquid suspensions containing photosensitive nanoparticles directly on the surface of a silicon ROIC reading and pre-processing photo signals without the use of microcontacts made of indium or other materials. Such photosensors use the frontal illumination, which distinguishes them from sensors based on epitaxial 3D materials, such as $In_{0.53}Ga_{0.47}As/InP$. In the latter photosensors, before being absorbed by the photosensitive layer ($In_{0.53}Ga_{0.47}As$) the radiation from objects in the viewed scene has to pass through a wide-band gap single-crystal substrate (InP) of the epitaxial layer, which is opaque to the visible region (0.4–0.76 μm), thus limiting the colour sensitivity of the photosensor to the wavelength range of 0.9–1.6 μm. Due to the possibility of using the frontal illumination of the photosensitive layer without the need for process operations aimed at thinning the substrates [7, 8], which greatly complicate the technology of manufacturing devices, the wide spectrality of QCD-based FPAs is ensured. For example, the use of PbS CQDs with colloidal quantum dots sized about 10 nm for making a photosensitive array layer enables registering the electromagnetic radiation within a wide spectral range of 0.4 to 2.1 μm [3].

The paper [9] describes the uncooled array photosensor 640×512 (15 μm pitch) developed by us for the spectral range of 0.4–2.0 μm and based on colloidal quantum dots PbS CQDs, where the electron-blocking hole transport layer was made of *p*-PbS-EDT CQDs (Fig. 1*a*).

This paper describes a new array photosensors (FPA) developed by us for the spectral range of 0.4–2.0 μm that features the 640×512 format and a pitch of photosensitive elements of 15 μm and is made of colloidal quantum dots PbS CQDs on the surface of the silicon ROIC reading *p*-channel photosignals. Unlike paper [9], here the electron-blocking layer (hole transport layer) is made of not liquid CQD suspension *p*-PbS-EDT, but of *p*-NiO_x material produced by magnetron sputtering. This material has recently started to be used for production of solar cells as a hole transport layer and has proven itself well due to its higher mobility and stability of properties as compared to organic materials [10, 11]. Other layers were made similarly to those in paper [9].

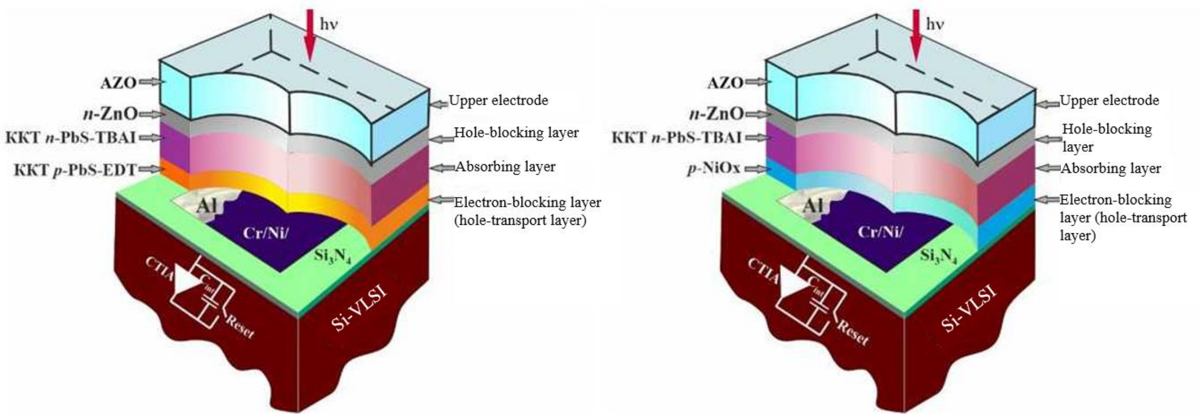

a) *b*)

Fig. 1. Architectures of FPA 640×512 (15 μm pitch) based on PbS CQDs: a) – FPA sensing element with the electron-blocking layer (hole transport layer) made of CQDs p-PbS-EDT [9]; b) – FPA sensing element with the electron-blocking layer (hole transport layer) made of p-NiO_x material

2. Architecture of array photosensor 640×512 with the electron-blocking and hole-transport layer based on *p*-NiO$_x$

The architecture of each photosensitive element developed by the authors of the new 640×512 array photosensor has the form Cr/Ni/*p*-NiO$_x$ CQD/*n*-PbS-TBAI/*n*-ZnO/AZO (Fig. 1*b*). The major part of photocarriers is generated by radiation in CQD layer *n*-PbS-TBAI. After photoexcitons decay, resulting electrons and holes are separated with the energy barrier of the *p*–*n* junction type at the contact of the *n*-PbS-TBAI CQD and *p*-NiO$_x$ CQD layers. The PbS CQD layer of the electron conductivity type is manufactured by substituting the initial ligand (oleic acid) after treatment with *tetra-n-butylammonium iodide*. *Lead chloride* and *N, N'-diphenylthiourea* are used as precursors of lead and sulfur in the synthesis of PbS CQD. The coating of zinc oxide doped with aluminum to form a solid solution in the ZnO-Al_2O_3 (AZO) system is used as a coating transparent for the electrode radiation [12].

The energy composition of the structure's individual layers that specifies the directions of electron and hole transport in the layers of the photosensor with the Cr/Ni/*p*-NiO$_x$/KKT *n*-PbS-TBAI/*n*-ZnO/AZO architecture is shown in Fig. 2*a* along with a similar energy composition of the layers of the Cr/Ni/KKT *p*-PbS-EDT/KKT *n*-PbS-TBAI/*n*-ZnO/AZO structure, which is shown in Fig. 2*b*.

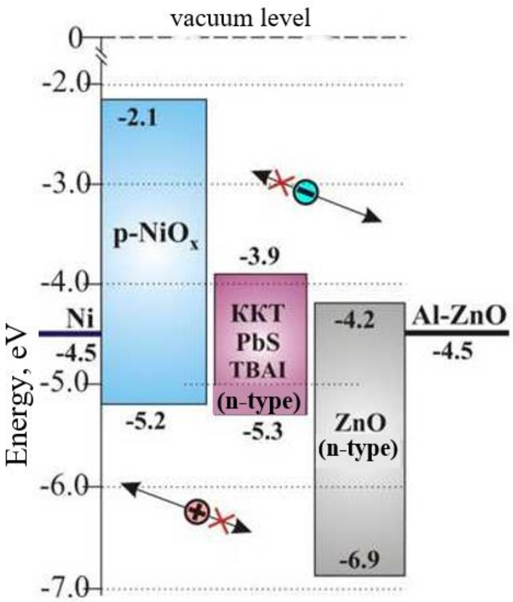

Fig. 2a. Energy composition of layers of the Cr/Ni/p-NiO$_x$/CQD n-PbS-TBAI/n-ZnO/AZO structure, on which basis array photosensor 640×512 made of PbS CQDs with the electron-blocking and hole-transport layer based on p-NiO$_x$ was developed

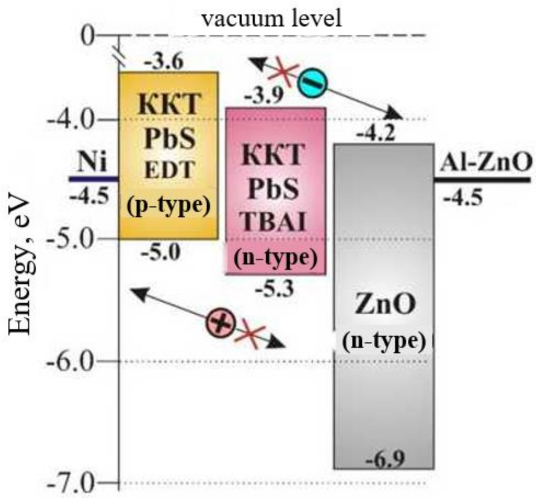

Fig. 2b. Energy composition of layers of the Cr/Ni/KKT p-PbS-EDT/KKT n-PbS-TBAI/n-ZnO/AZO structure, on which basis array photosensor 640×512 made of PbS CQDs with the electron-blocking and hole-transport layer based on PbS CQDs (p-EDT) [9] was developed

3. Properties of array photosensor 640×512 with the electron-blocking and hole-transport layer based on *p*-NiO$_x$

A photograph of the finished array photosensitive element of the 640×512 format based on colloidal quantum dots PbS CQDs with the silicon ROIC reading and pre-processing photo signals and an upper electrode made of Al:ZnO (AZO) mounted on the raster for research is shown in 3*a*.

The study of the spectral dependence of the optical absorption of the suspension of lead sulfide's colloidal quantum dots in the *n-octane* solution, that were synthesized by the above-described method using $PbCl_2$ as a lead precursor, showed the first exciton peak occurs with a maximum located at the wavelength $\lambda_{max} \approx 1.8$ μm. Its full width at half maximum (FWHM) was 220 nm, which indicates a sufficiently high monodispersity of PbS nanocrystals [13] in the absorbing layer of PbS CQDs (*n*-TBAI) of the finished array photosensor. Figure 3 shows the spectral dependence of the photosensitivity $S_i(\lambda)/S_i(\lambda_{max})$ reduced to unit for the array photosensor 640×512 with the silicon ROIC reading and pre-processing photo signals. The long-wave limit of photosensitivity is $\lambda_{lim} =$ $= 1.96$ μm, the width of the sensitivity band falls within the wavelength range of $\Delta\lambda =$ $= 0.4 \div 2.0$ μm. The use of the empirical relationship $E_0 = 0.41 + (0.025d^2 + 0.283d)^{-1}$ that was derived in paper [13] and establishes the connection between the energy of optical transitions E_0 in the optical absorption spectra of the CQD solution and diameter d of the nanoparticles showed that the diameter of the colloidal quantum dots we used is $d \simeq 9.5$–10 nm. The study of the nanoparticle shape by the high-resolution transmission electron microscopy showed that the prevailing CQD shape is a truncated octahedron (Fig. 4*a*). Each colloidal quantum dot has eight faces (111) and six faces (100), which is confirmed by the findings of the study conducted in [14]. The structure of faces (100) and (111) is shown in Fig. 4*b*. The photograph of CQDs obtained by the transmission microscopy method is shown in Fig. 4*c*.

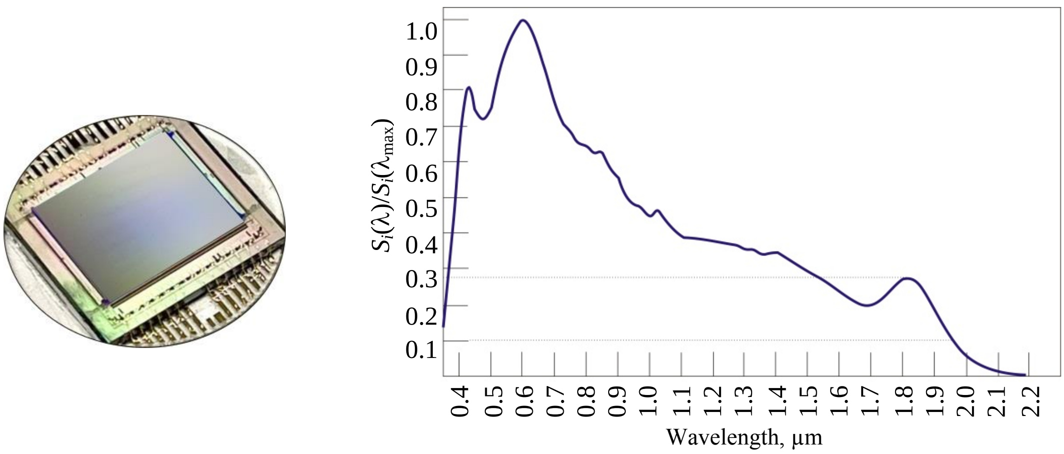

a) *b*)

Fig. 3. Array photosensitive element (PSE) of the 640×512 format based on colloidal quantum dots PbS CQDs with Cr/Ni/p-NiO$_x$/ККТ n-PbS-TBAI/n-ZnO/AZO architecture with silicon ROIC reading and pre-processing photo signals: a) – photo of raster-mounted PSE; b) – spectral dependence of photosensitivity reduced to unit at a room temperature

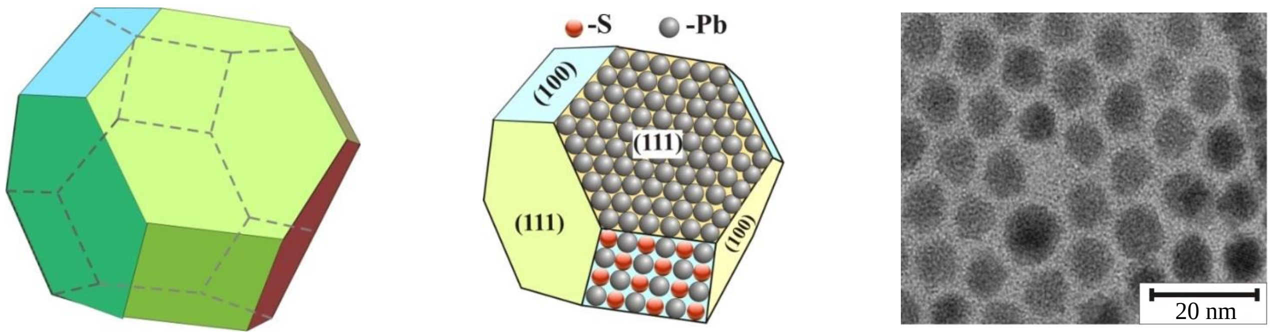

a) *b*) *c*)

Fig. 4. a) – model of the CQD shape (truncated octahedron); b) – composition of CQD nanocrystal faces (100) and (111); c) – photo of the CQDs obtained by the TEM method

The current-voltage characteristic of one of the photosensitive elements, which was measured at the room temperature in conditions of no illumination and under illumination from a monochromatic source with the wavelength of λ = 0.94 μm and a power P = 0.072 W·cm^{-2}, is shown in Figure 5. The current-voltage characteristics (CVC) have a form typical for structures with an energy barrier of the p–n junction type. The monochromatic ampere-watt responsivity at zero bias is S_0 = 0.35 A/W and increases to S_{-1} = 7.4 A/W at back bias equaling to V_{bias} = = -1.0 V. The average value of S_0 obtained by averaging the ampere-watt responsivity for 7 photosensitive elements is 0.27 A/W.

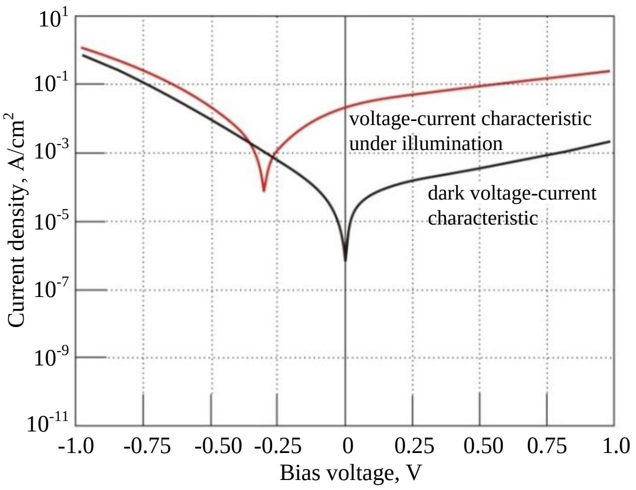

Fig. 5. Current-voltage characteristic of the photosensitive element under conditions of illumination from a monochromatic source (λ = 0.94 μm, P = 0.072 W·cm^{-2}) and in conditions of no illumination

The spectral dependence of the specific detectivity of the uncooled single-element photosensor with the Cr/Ni/p-NiO$_x$/KKT n-PbS-TBAI/n-ZnO/AZO architecture, which was measured under illumination from a black body with temperature T_{BB} = 1273 K at bias voltage V_{bias} equaling to 3.0 V is shown in Figure 6.

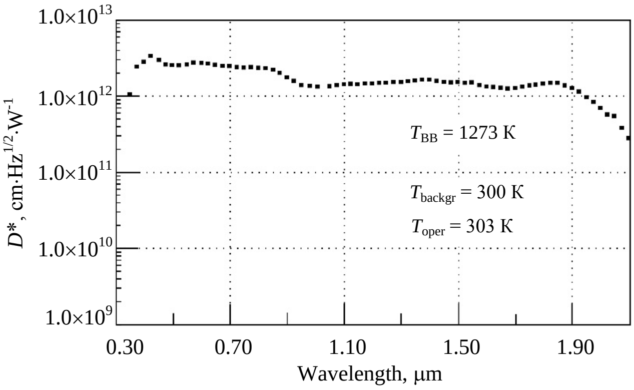

Fig. 6. Spectral dependence of the specific detectivity of the uncooled single-element photosensor with the Cr/Ni/p-NiO$_x$/KKT n-PbS-TBAI/n-ZnO/AZO architecture, which was measured under illumination from a black body with temperature T_{BB} = 1273 K (V_{bias} = 3.0 V)

Figure 7 shows fragments of images of the transportation assembly, hands holding a soldering iron and a human face that were made in the daytime under illumination of the viewed scene of 300–500 lux using the array photosensor 640×512 (15 μm pitch). Single-point correction and signal calibration using a defocused image were used.

a) *b*) *c*)

Fig. 7. Fragments of images made using the uncooled array photosensor 640×512 (15 μm pitch) based on colloidal quantum dots of PbS for the spectrum range of 0.4–2.0 μm; a) – transportation assembly (500 lux); b) – a hand holding a soldering iron (300 lux, $T_{soldering\ iron}$ = 300–350 °C); image of a human face (300 lux); given in brackets is the illumination of the scene when the photos were taken

4. Conclusion

The array photosensor 640×512 described herein and based on colloidal quantum dots of PbS features a photosensitivity range of 0.4–2.0 μm, which is expanded as compared to the devices based on the $In_{0.53}Ga_{0.47}As$ solid solution. The analysis of using such expanded photosensitivity area in night vision devices, which is detailed in paper [15], has shown:

a) the average value of natural night illumination in the absence of the moon within the wavelength range λ = 0.6–0.8 μm is (1.5–3.0)×10^{-5} W/n^2·μm, while within the wavelength range of 1.4–1.8 μm it increases to (6.0–7.0)×10^{-4} W/m^2·μm (Fig. 8);

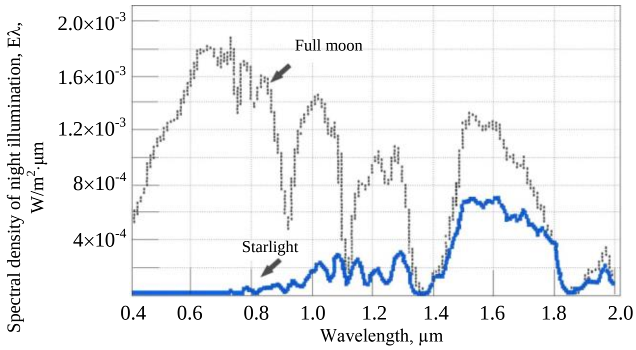

Fig. 8. Spectral density of night illumination under the full moon [16]

b) the atmosphere transparency of the near IR region is noticeably higher than in the visible region. Thus, within the meteorological viewing range of S_M = 10 km, the transmittance of the 1 km thick atmospheric layer at the wavelength λ = 0.6 μm is 0.72, and in the center of the transparency window of 1.4–1.8 μm it increases to 0.93;

c) atmospheric haze brightness decreases by more than 10 times within the wavelength range of 1.4–1.8 μm as compared to the visible region;

d) natural night illumination level within the spectrum range of 0.4–0.9 μm changes during the night from 10^{-1} W/m^2 to 2,5×10^{-5} W/m^2 (i.e. almost by 4 orders of magnitude), and within the spectrum range of 1.4–1.8 μm this change lies within the range of 1.6×10^{-1} W/m^2 to (3–4)×10^{-3} W/m^2;

e) contrast value (observed object/background) in the wavelength range of 1.4–1.8 μm is 1.4–1.5 times higher than within the range of 0.4–0.9 μm.

This proves the potential of using the array photosensors described herein that feature the expanded sensitivity range of 0.4–2.0 μm for the creation of advanced domestic night vision devices.

This work was supported by the Advanced Research Foundation.

REFERENCES

1. Popov V. S. and Ponomarenko V. P. New photosensorics: 0D vs 2D. Moscow, MIPT, 2024.
2. Ponomarenko V. P., Popov V. S., Shuklov I. A., Ivanov V. V. and Razumov V. F., Russ. Chem. Rev. **93** (4), RCR5113 (2024). https://doi.org/10.59761/RCR5113.
3. Hinds S., Klem E., Gregory C., Hilton A., Hames G. and Violette K., Proc. of SPIE **11407** (2020). https://doi.org/ 10.1117/12.2559115.
4. Malinowski P. E., Georgitzikis E., Maes J., Vamvaka I., Frazzica F., Van Olmen J., De Moor P., Heremans P., Hens Z. and Cheyns D., Sensors **17**, 2867 (2017). https://doi.org/10.3390/s17122867.
5. Gréboval C., Darson D., Parahyba V., Alchaar R., Abadie C., Noguier V., Ferré S., Izquierdo E., Khalili A., Prado Y., Potet P. and Lhuillier E., Nanoscale **14** (26), 9359–9368 (2022). https://doi.org/10.1039/D2NR01313D
6. Popov V. S., Ponomarenko V. P. and Popov S. V., Journal of Communications Technology and Electronics **69** (4–6), 219–226 (2024). https://doi.org/ 10.51368/1996-0948-2023-6-45-53.
7. Burlakov I. D., Grinchenko L. Y., Dirochka A. I. and Zaletaev N. B., Usp. Prikl. Fiz. (Advances in Applied Physics) **2** (2), 131–136 (2014) [in Russian].
8. Martin T., Dixon P., Gagliardi M.-A. and Masaun N., Proc. of SPIE **5726**, 85–91 (2005). https://doi.org/ 10.1117/12.596409.
9. Ponomarenko V. P., Popov V. S., Pankov M. A., Khamidullin K. A., Deomidov A. D., Fedorov A. A., Deev G. Yu., Dragunov D. E.,

Epifanov O. V., Lazarev P. S., Mirofyanchenko E. V., Ilyinov D. V., Petrushina V. A., Burlakov I. D., Polessky A. V., Startsev V. V., Brichkin S. B., Spirin M. G., Tovstun S. A., Gapanovich M. V., Gak V. Yu., Gadomska A. V., Pevtsov D. N., Katsaba A. V., Kirichenko A. S., Demkin D. V., Ivanova V. A., Ivanov V. V. and Razumov V. F., Applied Physics, No. 1, 45–54 (2025). https://doi.org/ 10.51368/1996-0948-2025-1-45-54.

10. Yin X., Guo Y., Xie H., Que W. and Kong L. B., Sol. RRL, 1900001 (2018). https://doi.org/ 10.1002/solr.201900001.

11. Lian X., Chen J., Shan S., Wu G. and Chen H., ACS Appl. Mater. Interfaces **12** (41), 46340–46347 (2020). https://doi.org/ 10.1021/acsami.0c11731.

12. Ajili M., Jebbari N., Turki N. K. and Castagné M., International Renewable Energy Congress 2010 (IREC2010, November 5–7, Sousse, Tunisia), pp. 305–309.

13. Moreels I., Lambert K., Smeets D., De Muynck D., Nollet T., Martins J. C., Vanhaecke F., Vantomme A., Delerue C., Allan G. and Hens Z., ACS Nano **3** (10), 3023–3030 (2009). https://doi.org/ 10.1021/nn900863a.

14. Beygi H., Abdolkarim Sajjadi S., Babakhani A., Young J. F. and van Veggel F. C. J., Applied Surface Science **457**, 1–10 (2018). https://doi.org/10.1016/j.apsusc.2018.06.152.

15. Gusarova N. I., Koshchavtsev N. F. and Popov S. V., J. Commun. Technol. **61** (10), 1211–1214 (2016).

16. Voilmerhausen R. and Maurer T., Proc. of SPIE **5076**, 60–69 (2003). https://doi.org/ 10.1117/12.487189.

About authors

Vladimir Pavlovich Ponomarenko, Chief Designer, Head of Department, Doctor of Physics and Mathematics, Professor, RD&P Center ORION, JSC (111538, Russia, Moscow, Kosinskaya Ulitsa, 9), Moscow Institute of Physics and Technology (National Research University) (141701, Russia, Moscow Region, Dolgoprudny, Institutsky Per., 9). E-mail: 2392325@gmail.com SPIN code 6882-8721, Author ID 171358

Viktor Sergeevich Popov, Head of the Center, Head of the Laboratory, Associate Professor, Candidate of Chemical Sciences, RD&P Center ORION, JSC (111538, Russia, Moscow, Kosinskaya Ulitsa, 9), Moscow Institute of Physics and Technology (National Research University) (141701, Russia, Moscow Region, Dolgoprudny, Institutsky Per., 9). E-mail: popov.vs@mipt.ru SPIN code 5846-8066, Author ID 862015

Mikhail Aleksandrovich Pankov, Head of Laboratory, Candidate of Physics and Mathematics, RD&P Center ORION, JSC (111538, Russia, Moscow, Kosinskaya Ulitsa, 9). E-mail: mpa.off@gmail.com SPIN code 7160-9289, Author ID 145651

Kamil Alievich Khamidullin, Group Leader, Department Head, RD&P Center ORION, JSC (111538, Russia, Moscow, Kosinskaya Ulitsa, 9). E-mail: kamil1986@list.ru SPIN code 4091-3295, Author ID 710558

Alexander Dmitrievich Deomidov, Leading Engineer, RD&P Center ORION, JSC (111538, Russia, Moscow, Kosinskaya Ulitsa, 9). E-mail:aleks.deomidov@mail.ru SPIN code 7744-0080, Author ID 760104

Artem Alekseevich Fedorov, Engineer Cat. 2, RD&P Center ORION, JSC (111538, Russia, Moscow, Kosinskaya Ulitsa, 9).

German Yuryevich Deev, Engineer Cat. 2, RD&P Center ORION, JSC (111538, Russia, Moscow, Kosinskaya Ulitsa, 9). E-mail: deew.german@ya.ru SPIN code 9119-4550, Author ID 1281139

Denis Eduardovich Dragunov, Engineer Cat. 1, RD&P Center ORION, JSC (111538, Russia, Moscow, Kosinskaya Ulitsa, 9). E-mail: dragunov-de@gmail.com SPIN code 9757-8370, Author ID 1234132

Oleg Vladimirovich Epifanov, Leading Engineer, RD&P Center ORION, JSC (111538, Russia, Moscow, Kosinskaya Ulitsa, 9).

Shamil Ilnurovich Zaripov, Leading Engineer, RD&P Center ORION, JSC (111538, Russia, Moscow, Kosinskaya Ulitsa, 9).

Pavel Sergeevich Lazarev, Leading Engineer, RD&P Center ORION, JSC (111538, Russia, Moscow, Kosinskaya Ulitsa, 9).

Ekaterina Vasilievna Mirofyanchenko, Group Leader, Candidate of Technical Sciences, RD&P Center ORION, JSC (111538, Russia, Moscow, Kosinskaya Ulitsa, 9). E-mail: mirofianchenko@gmail.com SPIN code 1825-9300, Author ID 1157308

Denis Vladimirovich Ilyinov, Engineer Cat. 1, RD&P Center ORION, JSC (111538, Russia, Moscow, Kosinskaya Ulitsa, 9). E-mail: dv.iljinov@physics.msu.ru SPIN code 2401-2262, Author ID 1033906

Victoria Alekseevna Petrushina, Process Engineer, RD&P Center ORION, JSC (111538, Russia, Moscow, Kosinskaya Ulitsa, 9).

Igor Dmitrievich Burlakov, Deputy Director General for Innovations and Science, Doctor of Technical Sciences, Professor, RD&P Center ORION, JSC (111538, Russia, Moscow, Kosinskaya Ulitsa, 9). E-mail: idbur@orion-ir.ru SPIN code 6042-3634, Author ID 171368

Aleksey Viktorovich Poleskiy, Chief R&D Designer, Candidate of Technical Sciences, RD&P Center ORION, JSC (111538, Russia, Moscow, Kosinskaya Ulitsa, 9). E-mail: av22236@BK.ru SPIN code 3992-4520, Author ID 571156

Vadim Valerievich Startsev, General Director, Candidate of Technical Sciences, RD&P Center ORION, JSC (111538, Russia, Moscow, Kosinskaya Ulitsa, 9). E-mail: orion@orion-ir.ru SPIN code 4028-7138, Author ID 942991

Sergey Borisovich Brichkin, Department Head, Chief Researcher, Doctor of Chemical Sciences, Moscow Institute of Physics and Technology (National Research University) (141701, Russia, Moscow Region, Dolgoprudny, Institutsky Per., 9), Federal Research Center for Problems of Chemical Physics and Medicinal Chemistry of the Russian Academy of Sciences (142432, Russia, Moscow Region, Chernogolovka, Academician Semenov Prospekt, 1). E-mail: brichkin@icp.ac.ru SPIN code 1534-8054, Author ID 44021

Maxim Gennadievich Spirin, Senior Research Assistant, Leading Research Assistant, Doctor of Chemical Sciences, Moscow Institute of Physics and Technology (National Research University) (141701, Russia, Moscow Region, Dolgoprudny, Institutsky Per., 9), Federal Research Center for Problems of Chemical Physics and Medicinal Chemistry of the Russian Academy of Sciences (142432, Russia, Moscow Region, Chernogolovka, Academician Semenov Prospekt, 1). E-mail: max2004@icp.ac.ru SPIN code 9434-0999, Author ID 54508

Sergey Alexandrovich Tovstun, Senior Research Assistant, Candidate of Physics and Mathematics, Associate Professor, Moscow Institute of Physics and Technology (National Research University) (141701, Russia, Moscow Region, Dolgoprudny, Institutsky Per., 9), Federal Research Center for Problems of Chemical Physics and Medicinal Chemistry of the Russian Academy of Sciences (142432, Russia, Moscow Region, Chernogolovka, Academician Semenov Prospekt, 1). E-mail: tovstun@icp.ac.ru SPIN code 6114-3430, Author ID 874253

Mikhail Vyacheslavovich Gapanovich, Senior Research Assistant, Candidate of Chemical Sciences, Moscow Institute of Physics and Technology (National Research University) (141701, Russia, Moscow Region, Dolgoprudny, Institutsky Per., 9), Federal Research Center for Problems of Chemical Physics and Medicinal Chemistry of the Russian Academy of Sciences (142432, Russia, Moscow Region, Chernogolovka, Academician Semenov Prospekt, 1). E-mail: gmw1@mail.ru Author ID 156921

Vladimir Yurevich Gak, Research Assistant, Candidate of Chemical Sciences, Moscow Institute of Physics and Technology (National Research University) (141701, Russia, Moscow Region, Dolgoprudny, Institutsky 9), Federal Research Center for Problems of Chemical Physics and Medicinal Chemistry of the Russian Academy of Sciences (142432, Russia, Moscow Region, Chernogolovka, Academician Semenov Prospekt, 1). E-mail: gak@icp.ac.ru SPIN code 6311-9408, Author ID 56719

Anna Vladimirovna Gadomskaya, Senior Research Assistant, Candidate of Chemical Sciences, Moscow Institute of Physics and Technology (National Research University) (141701, Russia, Moscow Region, Dolgoprudny, Institutsky Per., 9), Federal Research Center for Problems of Chemical Physics and Medicinal Chemistry of the Russian Academy of Sciences (142432, Russia, Moscow Region, Chernogolovka, Academician Semenov Prospekt, 1).

Dmitry Nikolaevich Pevtsov, Process Engineer, Junior Research Assistant, Moscow Institute of Physics and Technology (National Research University) (141701, Russia, Moscow Region, Dolgoprudny, Institutsky Per., 9). E-mail: pevtsov.dn@phystech.edu SPIN code 3117-5473, Author ID 1147563

Alexey Viktorovich Katsaba, Senior Research Assistant, Deputy Head of Laboratory, Candidate of Physics and Mathematics, Moscow Institute of Physics and Technology (National Research University) (141701, Russia, Moscow Region, Dolgoprudny, Institutsky Per., 9). E-mail: atsaba@sci.lebedev.ru SPIN code 5974-0289, Author ID 724698

Alexey Sergeevich Kirichenko, Senior Research Assistant, Candidate of Physics and Mathematics, Moscow Institute of Physics and Technology (National Research University) (141701, Russia, Moscow Region, Dolgoprudny, Institutsky Per., 9). E-mail: kirichenko@cosmos.ru SPIN code 9922-1027, Author ID 342444

Dmitry Viktorovich Demkin, Junior Research Assistant, Moscow Institute of Physics and Technology (National Research University) (141701, Russia, Moscow Region, Dolgoprudny, Institutsky Per., 9).

Valeria Antonovna Ivanova, Research Assistant, Candidate of Physics and Mathematics, Moscow Institute of Physics and Technology (National Research University) (141701, Russia, Moscow Region, Dolgoprudny, Institutsky Per., 9). E-mail: adu_99@mail.ru SPIN code 4277-9943, Author ID 1205481

Viktor Vladimirovich Ivanov, Director of the Institute of Quantum Technologies of Moscow Institute of Physics and Technology, Doctor of Physics and Mathematics, Corresponding Member of the Russian Academy of Sciences, Moscow Institute of Physics and Technology (National Research University) (141701, Russia, Moscow Region, Dolgoprudny, Institutsky Per., 9). E-mail: Ivanov.vv@mirt.ru SPIN code 1856-3914, Author ID 19128

Vladimir Fedorovich Razumov, Senior Research Assistant, Head of Laboratory, Doctor of Physics and Mathematics, Corresponding Member of the Russian Academy of Sciences, Moscow Institute of Physics and Technology (National Research University) (141701, Russia, Moscow Region, Dolgoprudny, Institutsky Per., 9). Federal Research Center for Problems of Chemical Physics and Medicinal Chemistry of the Russian Academy of Sciences (142432, Russia, Moscow Region, Chernogolovka, Academician Semenov Prospekt, 1). E-mail: azumov@icp.ac.ru SPIN code 1361-7759, Author ID 44050